AIAA Propulsion and Energy Forum
August 24-28, 2020, VIRTUAL EVENT
AIAA Propulsion and Energy 2020 Forum

10.2514/6.2020-3589

Conceptual Design of a 10-passenger Thin-haul Electric Aircraft

Boning Yang[1]
Rose-Hulman Institute of Technology, Terre Haute, Indiana, 47803

Fangyuan Lou[2] and Nicole L. Key[3]
Purdue University, West Lafayette, Indiana, 47907

With the development of battery technology, the all-electric airplane for thin-haul applications is becoming a reality in the upcoming decade. Compared to the traditional fossil-fuel-dependent airplanes, the electric-powered aircraft offers lower cost in terms of operation and maintenance and generates fewer greenhouse gases. The present study documents the effort in the conceptual design phase of a 10-passenger aircraft for thin-haul applications. According to the Federal Aviation Administration (FAA) regulations, the airplane falls into the category of general aviation. The range of the aircraft is 500nm VFR. It features a joint-wing design for better aerodynamic performance and is powered by two, newly designed, ducted propulsors. The maximum takeoff weight (MTOW) of the airplane is 15,400 lb, and the cruise speed of the aircraft is 245 KTAS (0.42 Mach) at an altitude of 30,000 ft. The takeoff and landing distances are 2200 ft and 1650 ft, respectively. To meet the range requirement, the battery weighs approximately 51% of MTOW using a pack level battery density of 300 Whr/kg, which is expected to be available at the early-to-mid 2020s.

Nomenclature

MTOW	= Maximum Take-off Weight	CTOL	= Conventional Take-off and Landing
EDF	= Electrical Ducted Fan	*KTAS*	= Knots True Airspeed
VFR	= Visual Flight Rules	IFR	= Instrument Flight Rules
AR	= Aspect Ratio	SPAN	= Wing Span, *ft*
PEF	= Performance Evaluation Function	C_{L_α}	= Lift-Curve Slope
C_L	= Lift coefficient	C_D	= Drag coefficient
α	= Angle of Attack (AOA.)	PWR	= Power-to-Weight Ratio
W/S	= Wing Loading		

[1] Mechanical Engineering Undergraduate Student, Mechanical Engineering, CM2030, 5500 Wabash Ave. Terre Haute, IN, 47803. Student Member AIAA.
[2] Research Scientist, School of Mechanical Engineering, 500 Allison Road.
[3] Professor, School of Mechanical Engineering, 500 Allison Road, Associate Fellow of AIAA.

Introduction

ELECTRIC propulsion has become one of the key emerging technology development areas in both academia and industry in recent years due to its unparalleled high energy efficiency, low operational cost, and minimal environmental impact compared to traditional propulsion systems that use fossil fuels. For the thin-haul mission, using an all-electric propulsion system instead of the conventional turboprop can save up to 84% of energy costs (fuel), and an overall 31% reduction of total operational costs from energy cost alone [1]. Operational cost The electric propulsion system can also significantly reduce the emission of incomplete combustion products and noise for both in the cabin and on the ground. The International Air Transport Association (IATA) sets a goal to reduce the net CO_2 emission of aviation in 2050 by 50% compared to 2005 levels, and also a cap on net aviation CO_2 emission from 2020 [2]. Based on the United Nation's International Civil Aviation Organization's estimation, such a reduction is impossible to achieve without the application of sustainable aviation fuels [3]. Therefore, electric propulsion is one of the most promising solutions to achieve the emission reduction goal of IATA. Although electric propulsion has been in use for unmanned aerial vehicles (UAV) and model airplanes, the progress toward manned electric aircraft has been slow primarily due to the constraint of battery technology. Significant progress has been made in recent years using different types of electric propulsion systems, and several successful flight demonstrators have used batteries, hybrid systems, fuel cells, turboelectric systems, or even solar cells as power sources [4]. However, none of the flyable manned electric aircraft can achieve sufficient mission performance, in terms of both capacity and range, to compete with the in-service aircraft of similar sizes. Batteries have been the major limiting factor for the application of electric propulsion on aircraft, as they have much lower specific energy than jet fuels.

However, a recent study conducted by NASA Glenn Research Center estimated that a 300 Wh/kg specific density of battery at pack energy density level is achievable as early as 2022-25 without extra investments [5]. Thus, the all-electric airplane for thin-haul applications is realistic for the 2020s with the current aircraft technology. A study showed that electric aircraft could have a significant energy benefit for flights with ranges under 1000 nm [6] in applications such as air taxis, commuter planes, etc. In the meantime, several companies and organizations already started designing Conventional Takeoff and Landing (CTOL) airplanes using electrified propulsors based on current technology for thin-haul missions. For instance, two start-up companies, Eviation and Zunum Aero, have started the design of all-electric or hybrid-electric airplanes [7, 8], shown in Figure 1. Both airplanes fall in the category of general aviation airplanes, with a target range of around 700 miles. The capacity of both airplanes is approximately ten passengers. However, the all-electric design, Eviation Alice, has a battery weight percent of 60% [7], which is significantly higher compared to a typical range of 20% to 30% fuel weight for the conventional thin-haul aircraft.

Despite the increased attention to all-electric airplanes, new design challenges, such as the balance of battery weight and range, integration of electric propulsors, are encountered. In the present study, the conceptual design of a 10-passenger Thin-haul Electric Aircraft (TEA-10) was completed using battery technology achievable in the late 2020s.

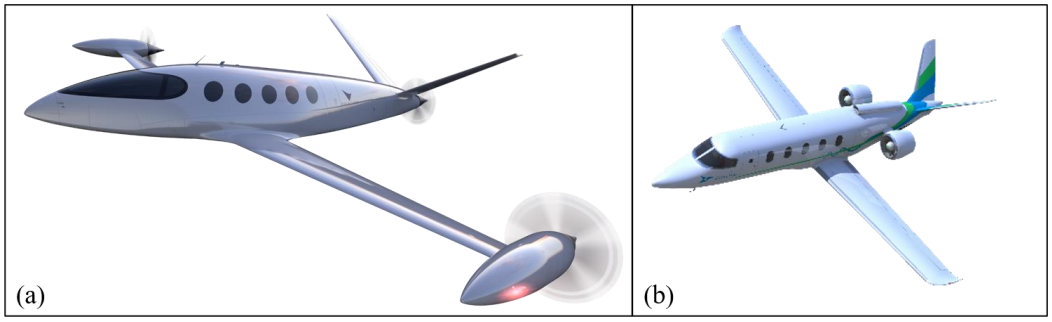

Figure 1: Picture of Eviation Alice (a) and Zunum Aero ZA10 (b), according to Refs. 7 and 8.

I. Mission Requirements, Benchmarking, and Regulations and Constraints

A. Benchmarking

The electric airplane in the present study is targeting the market of light regional jet and turboprop airplanes. To understand its competitors in the market, five designs were selected as benchmarking targets, including three conventional fossil-fuel-powered airplanes, and two electric or hybrid-electric designs. Those five benchmarking targets are chosen because they have similar passenger capacity and represent different popular configurations for thin-haul aircraft. Pilatus PC12 is one of the most popular single-engine turboprop business aircraft on the market. Single-engine turboprop aircraft are usually smaller and lighter compared to competitors with different configurations. Correspondingly, they are typically cheaper to operate but also have a smaller cabin. The Pilatus PC24 is a light business jet. It has a greater range and significantly higher cruising speed compared to PC12. Also, it is heavier due to its more complex system, and it is more expensive to operate because of the utilization of jet engines. Beechcraft King Air 350i is the modern version of the bestselling turboprop aircraft. Compared to the PC12 with a single turboprop engine, the twin turboprop configuration allows more maximum takeoff weight and more spacious cabin space. In addition, the full electric Eviation Alice and hybrid Zunum ZA-10 were also included in the benchmarking targets. A list of their primary parameters is shown in Table 1.

Table 1: Benchmarking Table

	Zunum ZA10	Eviation Alice	PC12 NG [9]	PC24 [10]	King Air 350i [11]
Capacity	10+2	9+2	9+2	8+2	9+2
Range [nm] (Max Loading)	610	540	1,803	2,000	1,806
Cruising Speed [KTAS]	295	240	285	440	312
MOTW [lb]	11,500	14,000	10,450	18,300	15,000
Propulsor	Twin EDF	Triple Electric Propellers	Single Turboprop	Twin Turbofans	Twin Turboprops
Energy Pack Weight Percent	20% Battery 7% Fuel	60% Battery	26% Fuel	33% Fuel	24% Fuel

B. Mission Requirements

The capacity of the thin-haul electric airplane, TEA, is set to be 10-passengers plus 2 flight crews, which is comparable to the capacity of the benchmarking targets. The operational range for the TEA was selected to be 500 nm under Visual Flight Rules (VFR) condition. Although 500 nm is lower than the operational range of the conventional fossil-fuel-based counterpart airplanes in the market (such as PC12 and PC24), it is sufficient for most thin-haul missions, which are typically less than 300nm according to Ref. 1. Figure 2 shows the range maps of 500 nm from Washington DC, Los Angeles, and Frankfurt. A range of 500 nm allows connections to major cities such as Washington DC-Atlanta, Los Angles - San Francisco – Phoenix, Frankfurt – London, or Paris – Warsaw. In addition, the range also meets most on-demand transportation needs or special missions, such as emergent medical services. A minimum cruise speed of 200 KTAS is required to be categorized as general aviation aircraft. Lastly, the maximum takeoff and landing distances were set to be 2,500 ft and 2,000 ft, respectively, which allows the airplane to operate at most airports.

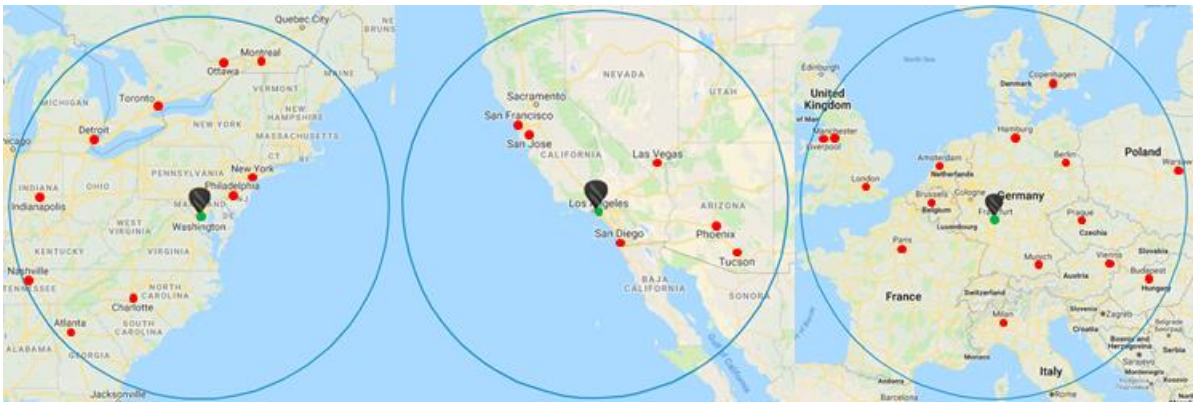

Figure 2: Range map shows of 500 nm from Washington DC (left), Los Angeles (middle), and Frankfurt (right).

C. Regulations and Constraints

The design of this airplane follows the regulations of the Federal Aviation Administration (FAA). Part 23 in Title 14 CFR regulates the airworthiness standards for normal category airplanes [12] and is the main regulation for airplanes in the present study. Based on the passenger capacity of the TEA, it is classified as a Level 4 High-speed aircraft. The MTOW of TEA shall be less than 19,000 lb to be classified as normal category airplanes. The airplane's performance should follow the requirements in Subpart B of Part 23. Subpart C of Part 23 specified the Structures requirements, and the limits and ultimate loads are specified in §23.2230. The mission requirements for commuter and on-demand operations are documented in Part 135 in Title 14 CFR, in which subpart D covers the operation limitations and weather requirements of Visual Flight Rules (VFR)/Instrument Flight Rules (IFR). It is worth noting that both VFR and IFR operations require a fuel reserve of 30 minutes (during the day, VFR) or 45 minutes (IFR or during night VFR) at normal cruising speed, which will be shown to be a challenge in the design of a thin-haul electric airplane.

II. Roadmap of the Conceptual Design

Figure 3 shows the roadmap for the conceptual design of the electric airplane in the present study. The design process follows Raymer's procedure [13]. With the information from mission requirements, benchmarking, and constraints, the procedure starts with an initial sizing of the airplane. Typically, the initial sizing of the airplane is conducted by considering the dimensions of the benchmarking targets and other airplane's historical data. These initial dimensions will be used for structural weight and aerodynamics estimations. The process can take a few iterations until all the constraints were met. Lastly, a trade study is conducted to find an optimized design solution.

In the present study, a new dimensionless parameter, Performance Evaluation Function (PEF), was developed to gauge the performance of an electric airplane in the trade study. It is described as:

$$PEF = \frac{MTOW \times {W_{batt}}^{0.8} \times TO^{0.2}}{n^{0.2} \times NPASS \times VCMN^{0.6} \times \frac{(WSR \times CH)^{0.2}}{100}} \quad (1)$$

where, $MTOW$ is the maximum takeoff weight, TO is the takeoff distance at the dry paved runway, W_{batt} represents the battery weight as a percentage of the total weight, n is the designed loading factor, $NPASS$ is the number of passengers, $VCMN$ is the cruising speed, WSR is the wing loading factor, and CH is the cruising altitude. With the inclusion of these parameters, the value of PEF reflects the performance of the airplane. For instance, the maximum takeoff weight and battery weight are critical for the certification and challenges of design. Takeoff distance is essential for the airplane to be able to operate on more runways, while the maximum sustainable loading factor is directly related to the turning radius. The number of passengers and cruising speed is critical for the operations. The wing loading and cruising altitude are directly related to the comfort of the airplane: the higher the wing loading and cruising height are, the smoother the ride will feel to the passengers. In the trade study, the design parameters are adjusted to minimize the value of PEF.

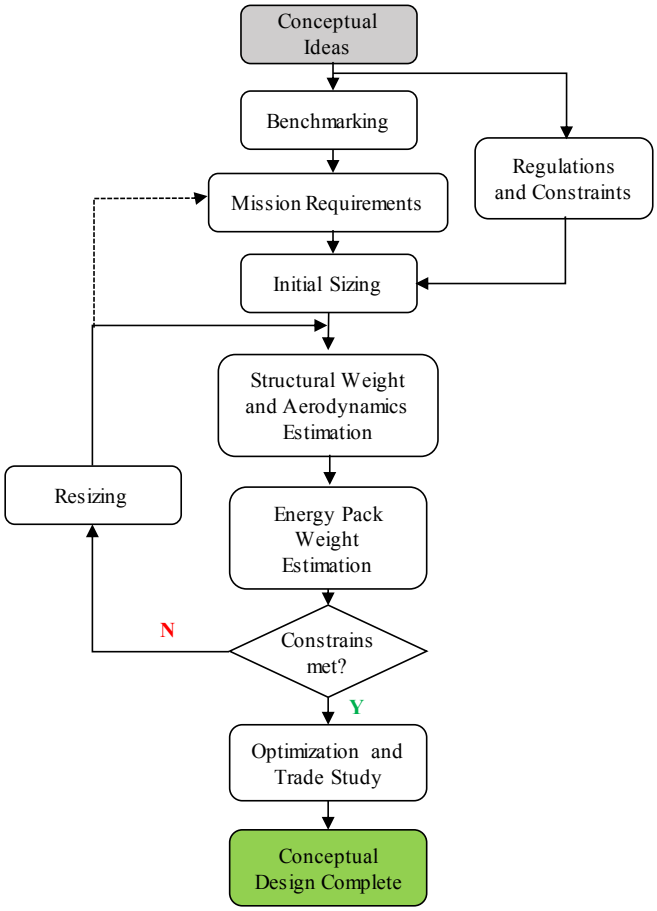

Figure 3: Roadmap for Aircraft Conceptual Design.

III. Results

A rendering of the final design of the thin-haul electric airplane is shown in Fig. 4a. In addition, Fig. 4b shows the three-side view with major dimensions indicated. The airplane falls in the category of general aviation, according to FAA regulations. The airplane employs a low-wing configuration with a wingspan of 59.6 ft. In addition, a combined V-tail and joint wing configuration were selected for the benefits of aerodynamic performance. The aircraft is powered by two, full-electric, ducted fans mounted at the rear section of the fuselage. The range of the aircraft is 500nm VFR. The MTOW of the airplane is 15,400 lb, and the cruise speed of the airplane is 245 KTAS (0.42 Mach) at an altitude of 30,000 ft. The takeoff and landing distances are 2500 ft and 1650 ft, respectively. The capacity of the airplane is ten passengers with a maximum payload of 2,000 lb. The travel time is less than 150 minutes. A list of critical parameters for TEA is shown in Table 2.

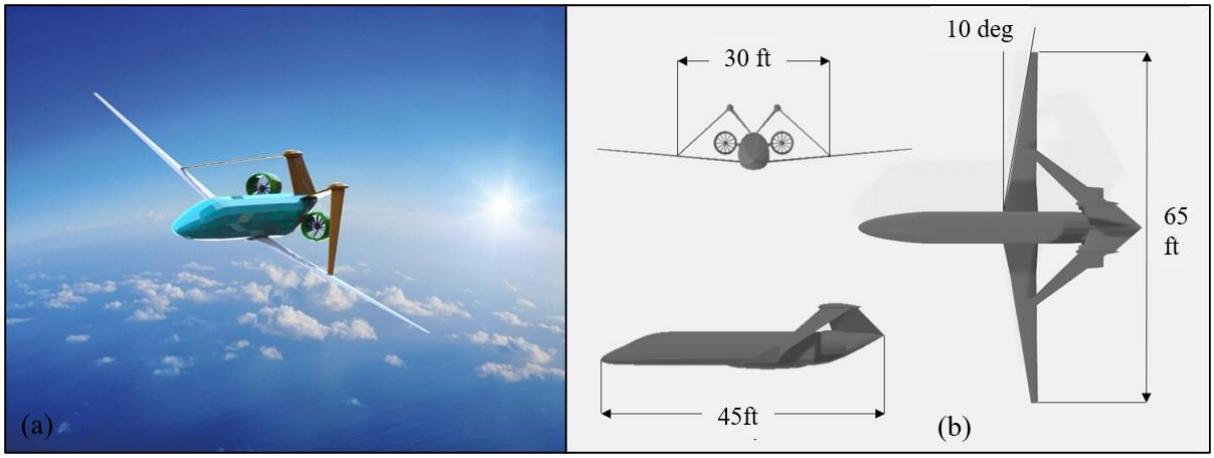

Figure 4: Rendering Picture (a) and three-side view (b) of TEA.

Table 2: Key Specifications of the Thin-Haul Electric Airplane.

Fuselage Length: 45 *ft*	Wing Span: 65 *ft*
Maximum Capacity: 10 passengers + 2 crews	Maximum Take-off Weight: 15,400 lb
Main Wing Aspect Ratio: 15	Main Wing Leading Edge Sweep Angle: 10 degree
Main Wing Taper Ratio: 0.2	Wing Loading Ratio: 65 lb/ft^2
Cruising Speed: 245 KTAS	Cruising Altitude: 30,000 *ft*
Stall Speed: 93 KTAS	Maximum Climb Rate: 1,905 ft/min
Maximum Speed: 304 KTAS	Maximum Payload: 2,000 lb

A. Configuration Selection

The configuration includes: 1) fuselage dimensions, 2) wing shape, 3) engine locations, and 4) tail configurations. In the present study, a tool called OpenVSP, a free parametric aircraft geometry tool developed by Gloudemans *et al.* [14], is used to sketch the airplane during the conceptual design phase.

1) Fuselage Dimension Selection

The dimensions of the fuselage were selected to be 45-ft in length, 5-ft in width, and 5.3 ft in depth. These dimensions are similar to those of benchmarking airplanes. Also, the length of the passenger compartment, XLP, was determined to be 20 *ft*. Those dimensions are determined based on information on the cabin layout and sizes for several commercial airliners as well as airplane interior data from Fielding's [15]. It falls in the range of PC12NG and PC24, which is shorter than PC24 but longer than PC12NG. Thus, the electric airplane in the present study shall provide a comparable level of comfort to its competitors. A schematic passenger compartment layout of 10 seats and the cross-section is shown in Fig. 5. Though not shown here, other layout plans are also available for other applications such as mail delivery and air ambulance.

2) Wing Selection

The parameters concerning the wing design include: 1) wing loading factor, WSR, 2) aspect ratio, AR, 3) taper ratio, TR, and 4) leading-edge sweep angle. The selection of the wing loading factor requires a balance of wing area and stress level. A small wing loading factor can result in an increase in aircraft weight and drag due to the excessive wing area. On the other hand, a high loading factor can significantly limit the design space, primarily due to sustained loading constraints and landing requirements. In the present study, a medium wing loading factor of 65 lb/ft^2 was selected. This wing loading falls into the range of the wing loading for most civil aircraft of similar size. In addition, the aspect ratio, taper ratio, and leading-edge sweep angle of the main wings were set to be 15, 0.2, and 10 degrees, respectively. The maximum thickness, *tmaxc*, defined as the ratio of the maximum thickness to the chord, was set to be 0.05. Lastly, the critical Angle of Attack (AOA) of the wing was set at 15 degrees.

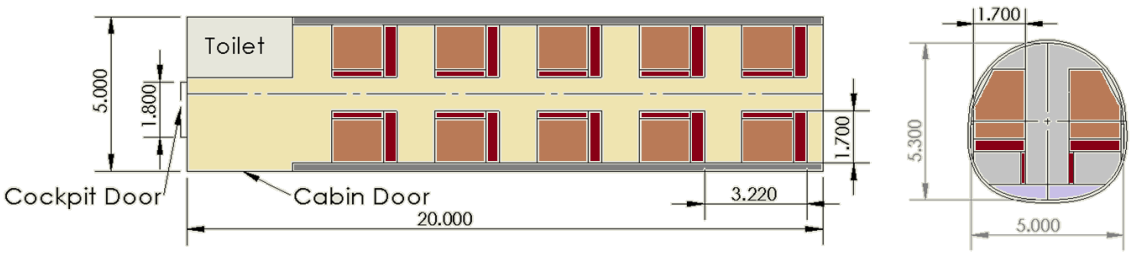

Figure 2 Schematic Layout of the passenger compartment for TEA, all dimensions are in *ft.*

3) Engine Selection, Location, and Mounting

The power unit for this aircraft is two Electric Ducted Fans (EDF) [16]. Each propulsor is expected to have a 500 kW power output and produces a maximum thrust of 1800 lb. The diameter of the ducted fan is approximately 40 inches. The design mass flow rate is on the order of 250 lb/s, and the target isentropic efficiency of the duct fan is 90%. The weight for each EDF is estimated to be approximately 500 lb using the equations developed by Dowdle et al. [17] for preliminary sizing of ducted fans. Both ducted fans are designed to be mounted at the rear section of the fuselage instead of under the wings for three reasons:

1. It reduces the landing gear height, which allows the operation of the airplane at airports with limited ground support;
2. It reduces the cabin noise level;
3. It eliminates the risk for the potential damage of the passenger compartment due to severe engine failure.

It is also worth noting that the choice of the rear mounting location will make the stability and balance more challenging since a significant amount of weight will be loaded at the rear part of the airplane, which may require exercising the distribution of batteries and other systems to counteract the weight of the ducted fans.

4) Tail Configuration and Joint Wing Integration

A V-tail configuration was selected for the electric plane in the present study because of the benefit of lower drag at the tail of the airplane. In addition, the V-tail configuration provides enough clearance for the installation of the electric ducted fans, the dimensions of which are significantly larger than those on conventional turbojet engines. Also, a joint wing design was selected for better aerodynamic performance based on the findings from previous studies. For instance, studies conducted by Cuerno-Rejado et al. [18] and Garica-Benitez et al. [19] showed the potential benefits of joint-wing design compared to conventional design, including lower structural weight, reduced induced drag, and larger range with the same amount of payload. The study by Garica-Benitez et al. [19] showed a 20% reduction in empty weight, an overall drag reduction of 8.13%, and a 6.7% increase in lift-to-drag ratio at cruise with the implementation of a joint wing. The increased lift-to-drag ratio at cruise led to an increased range with the same fuel capacity. The implementation of a joint wing design can result in a reduced fuel tank capacity for fossil fuel-dependent airplanes. However, this is not an issue for the electric airplane in the present study since the battery pack is placed in the fuselage.

The integration of the joint wing design requires a detailed analysis of its influences on structural and aerodynamic performance. In the phase of conceptual design, the typical approach is to start with a conventional design and then integrate the joint-wing design by applying factors based on previous research findings. In the present study, the joint-wing design does not change the total wing area, which is the same as in Ref. 19's study. The primary wing (front wing) and aft wing are designed to provide 85% and 15% percent of total lift. Considering that the size of TEA-10 is smaller than the airplane studied in Ref. 19, the reduction in empty weight attributed to the joint wing was estimated to be 15%. The total reduction in drag is roughly expected to be 10%, and the resulted benefit in the lift-to-drag ratio is 7.8%. This is a higher drag reduction compared to the results in Ref. 19, but still reasonable.

B. Weight Estimation

The total weight of TEA consists of three parts: 1) structural and equipment weight or so-called 'empty weight,' 2) energy pack weight or battery weight in the present study, and 3) payload weight.

$$W_{tot} = W_{emp} + W_{batt} + W_{payload} \tag{2}$$

1) Structural and Equipment Weight Estimation

The structural weight of the TEA was estimated following the procedure in the Flight Optimization System (FLOPS) by NASA. [20]. FLOPS was developed at NASA Langley Research Center as a design tool for aircraft conceptual design. It is capable of weight estimation, aerodynamic analysis, propulsion system scaling, mission analysis, takeoff/landing estimation, cost analysis, and noise prediction. Over the years, the weight estimation procedure has been shown to be very reliable and adopted in the present study. Figure 6 shows the breakdown of the empty weight for TEA-10. The estimated values are within the range suggested by Torenbeek [21]. The differences between the results and Torenbeek's data were considered reasonable since Torenbeek's data were extracted from aircraft in the 1980s. For TEA-10, the heaviest structural component is the wing, which takes up to 19% of the overall empty weight. In addition, the ducted fans, fuselage, and landing gear take 16%, 15%, and 10% of the total empty weight of the aircraft, respectively. Furnishing account for 14% of the total empty weight. Electrical and Avionics use 11% and 5% of the total weight, respectively. Lastly, the weight of the control surface, instruments, air conditioning, and anti-icing equipment were included in the miscellaneous (Mics) category, which is estimated to be 9% of the

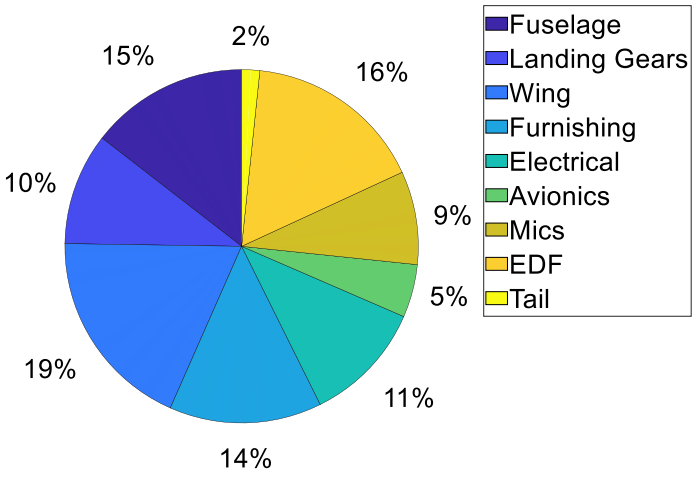

Figure 6: Total Empty Weight Break Down for TEA.

overall aircraft empty weight. Though not presented here, the detailed procedure for weight estimation can be found in Appendix A.

2) Payload Weight Estimation

According to CFR §135.99, two pilots are required to operate TEA. However, no flight attendant crewmember is required based on the operation range, cruising speed, and the maximum flight time (less than two hours and a half), according to CFR §135.107. Therefore, the payload of TEA includes two pilots and ten passengers. According to FLOPS, each flight crew member's average weight, including the luggage, is 225 lb. The average weight for a passenger is 200 lb, with the inclusion of 35 lb for luggage. Therefore, the overall payload for TEA is approximately 2,450 lb, obtained from:

$$W_{payload} = 2 \times 225\ lb + 10 \times (165 + 35)\ lb = 2450\ lb \tag{3}$$

3) Battery Weight Estimation

The battery provides all the energy required for the operation of TEA. With a specific mission profile, the estimation of its weight is based on the conservation of energy. For thin-haul electric aircraft in the present study, the flight mission can be categorized into four phases: takeoff, climbing, cruise and loitering, and landing. It is worth noting that the energy required during the landing phase is not included in the present analysis because the aircraft gains energy with the descending of altitude. In addition, the energy needed during loiter is treated as an extension of range requirements at cruise speed. For instance, for an airplane with a designed operational range of 100 nm and the loiter of 30 mins at a cruise speed of 100 KTAS, the total energy required with loiter is the same as the energy required for the operation of 150 nm at cruise speed. The energy needed at different phases was converted into the ratio of battery weight with respect to MTOW. A 300 Wh/kg specific battery density (pack level) was used in the analysis.

The battery energy ratio required for takeoff, $BATTR_{TO}$, is described as:

$$BATTR_{TO} = \frac{1}{\eta_{EDF} \times C_{batt}} \times \left[\frac{1.44 \times (WSR)}{\rho_{GD} \times g \times C_{L_{max,TO}}} + \frac{1.44 \times C_{D0} \times S_{TO}}{2 \times C_{L_{max,TO}}} + \mu_{RTO} \times S_{TO}\right] \tag{4}$$

where, η_{EDF} is the isentropic efficiency of the electric duct fan, ρ_{GD} is the local air density at the takeoff location, S_{TO} is the takeoff distance, and μ_{RTO} is the rolling resistance from landing gear at takeoff (set as 0.02 for analysis). The calculation covers only the energy required to accelerate the aircraft to lift-off speed on the runway, and μ_{RTO} is subject to change with different runway conditions, such as wet/dry, paved/unpaved, etc.

The battery energy ratio required for climbing, $BATTR_{CL}$, is expressed as:

$$BATTR_{CL} = \frac{\Delta h}{C_{batt}} \times \frac{P_{EDF}}{W_{tot}} \times \frac{1}{ROC_{max}} \tag{5}$$

where Δh is the height of climb which is 30,000 ft from sea-level to the cruising altitude, P_{EDF} is the maximum power output of the electric duct fan, and ROC_{max} is the maximum climb rate.

Lastly, the battery energy ratio required for cruising and loiter, $BATTR_{CRU}$, is:

$$BATTR_{CRU} = (R + T_{LO} \times a_{CMN} \times V_{CMN} - R_{CL}) \times (\frac{1}{LD_{max}}) \times \frac{1}{\eta_{EDF} \times C_{batt}} \tag{6}$$

where R is the designed operating range which is 500 nm. for TEA, T_{LO} is the required loiter flight time, a_{CMN} is the local speed of sound at the cruising altitude, and R_{CL} is the distance traveled during climbing.

Therefore, the overall battery weight ratio is obtained:

$$BATTR_{TOT} = BATTR_{CRU} + BATTR_{TO} + BATTR_{CL} \tag{7}$$

Furthermore, the total weight of the aircraft or maximum takeoff weight (MTOW) is:

$$MTOW = \frac{W_{emp} + W_{payload}}{1 - BATTR_{TOT}} \tag{8}$$

The calculation of the overall weight ratio and MTOW is an iterative process. An initial guess of $MTOW$ is used in Eqn. (5) and also to estimate W_{emp} , and then it is updated with the value obtained from Eqn. (8). The results were considered converged if the differences in the calculated $MTOW$ from the previous two iterations were within 0.05%.

4) Total Weight Breakdown

Figure 7 shows the total weight or MTOW breakdown for TEA. The MTOW for TEA is 15,400 lb. The heaviest component of aircraft is the battery pack. To meet the range requirement of 500 nm VFR, the weight of the battery is approximately 51% of the MTOW of the aircraft. The structural weight takes 20% of MTOW. The payload of the aircraft, which includes both passengers and their luggage, is approximately 16% of the MTOW.

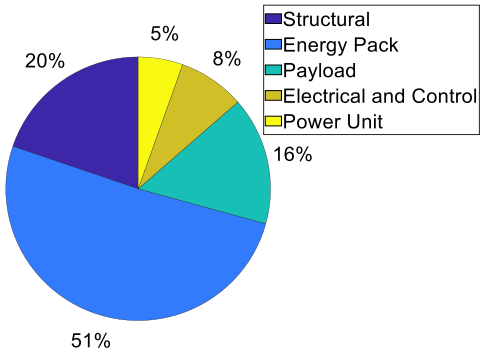

Figure 7: Total Take-Off Weight (MTOW) Break Down for TEA.

C. Aerodynamic Analysis

The aerodynamic analysis of an airplane includes the estimation of lift and drag coefficients and critical Mach number. Evaluation of these parameters was based on equations provided by Brandt et al. [22] and Raymer [13] using mainly wing geometry. The equations used in the present study are simplified but provide a good estimation to roughly predict the performance of the aircraft during the conceptual design phase.

1) Estimation of Lift and Drag Coefficient

Since TEA is designed to fly at the subsonic region, the lift-curve slope, C_{L_α}, can be estimated with information on wing configurations. It is calculated with:

$$C_{L_\alpha} = \frac{2\pi AR}{2+\sqrt{4+\frac{AR^2\times\beta^2}{0.95^2}(1+\frac{tan^2\Lambda_{\max t}}{\beta^2})}} \times \frac{0.98\pi}{180} \tag{9}$$

where AR is the aspect ratio of the wing, $\Lambda_{\max t}$ is the sweep angle of the wing at the chord location of maximum thickness, β is calculated as $\beta^2 = 1 - VCMN^2$, and $VCMN$ is the cruising speed of TEA-10.

Furthermore, the maximum lift coefficient at different conditions is obtained using:

$$C_{L_{max,no\ flap}} = C_{L_\alpha} \times (\alpha_{stall} - \alpha_{L=0}) \tag{10}$$

$$C_{L_{max,TO}} = C_{L_{max,no\ flap}} + C_{L_\alpha} \times 10^\circ \times SFS \times \cos(\Lambda_{TE}) \tag{11}$$

$$C_{L_{max,LD}} = C_{L_{max,no\ flap}} + C_{L_\alpha} \times 15^\circ \times SFS \times \cos(\Lambda_{TE}) \tag{12}$$

where, $C_{L_{max,no\ flap}}$ is the maximum lift coefficient with no-flap extended, $C_{L_{max,TO}}$ is the maximum lift coefficient during takeoff with a flap extended at 10°, and $C_{L_{max,LD}}$ is the maximum lift coefficient during landing with a flap extended at 15°. Flap area ratio (SFS) is defined as the area of the flaps versus the reference wing area. Its value was set to be 0.35 for TEA. α_{stall} is the stall angle of the airplane, and its value is 15° for TEA. $\alpha_{L=0}$ is the zero-lift angle of attack for the airplane, and its value is approximately -2°. Lastly, Λ_{TE} is the trailing edge sweep angle, which can be extracted from the wing geometry.

In addition, the lift coefficient at minimum drag is obtained using:

$$C_{L_{min\,D}} = C_{L_\alpha} \times (\frac{-\alpha_{L=0}}{2}) \tag{13}$$

The drag coefficient of the airplane is estimated using:

$$C_D = C_{D0} + k_1 \times {C_L}^2 + k_2 \times C_L \tag{14}$$

where the descriptions of C_{D0}, k_1, and k_2 are:

$$C_{D0} = C_{f_e} \times SWS + k_1 \times {C_{L_{min\,D}}}^2 \tag{15}$$

$$k_1 = \frac{1}{\pi \times e_0 \times AR} \tag{16}$$

$$k_2 = -2 \times k_1 \times C_{L_{min\,D}} \tag{17}$$

The equivalent skin-friction coefficient (C_{f_e}) was selected to be 0.004 for TEA, SWS is the wetted area of TEA-10, which is estimated using aircraft dimensions.

The improvements of the joint wing are then applied to the drag coefficients accordingly. A variety of lift coefficients were exercised in the conceptual design to find the maximum value of the lift-to-drag ratio. The value of the lift-to-drag ratio is a critical measure of the aerodynamic performance of an airplane. A larger lift-to-drag ratio is usually more favorable in aircraft design since it usually leads to better fuel economy and climbs performance. The maximum lift-to-drag ratio is used to determine the optimized cruising speed in this study. It's also worth noting that the drag coefficient estimation is only valid at speeds lower than the Critical Mach Number.

2) Calculation of Critical Mach No.

Critical Mach number (MCRIT) is needed to set the maximum speed and to determine the appropriate cruising speed of the airplane. Aircraft should not exceed the Critical Mach number to avoid the dramatically increased drag. In the present study, the critical Mach number for TEA is estimated using:

$$MCRIT = 1.0 - 0.065 \times (100 \times tmac)^{0.6} \times cos^2 \Lambda_{LE} \tag{18}$$

where, $tmac$ is the ratio of the maximum thickness to chord, and Λ_{TE} is the leading-edge sweep angle of the wing. TEA-10 has an MCRIT determined as Mach 0.83, and the maximum speed of TEA-10 is designed as Mach 0.51 at cruise elevation.

D. Mission Analysis.

In the mission analysis, the mission profile is separated into four phases: takeoff, climbing, cruising/loiter, and landing, shown in Fig. 8. The energy consumption for each phase was also indicated in the figure. As expected, most energy, 76.7%, is consumed during cruise and loiter. Climbing consumes 22.9% of the total energy, and takeoff only

consumes 0.4% of the total energy. In addition, the power requirements for each are also listed in Table 2. The maximum power is required for operation at a sustained loading flight of 1.95 g, nearly the maximum available power (94%). Takeoff requires approximately 92% of maximum available power while cruising only requires 38% of the

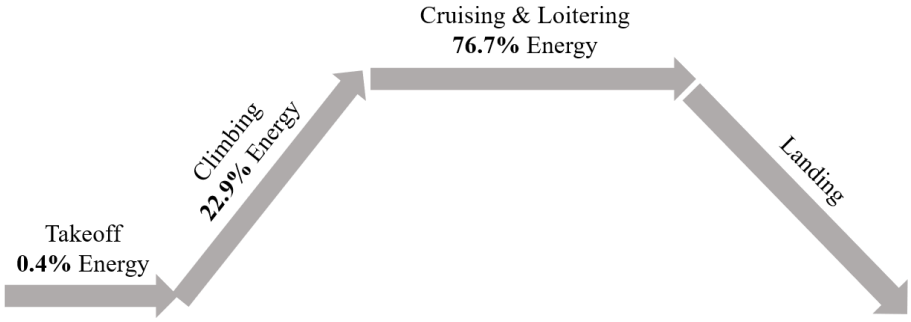

Figure 8: Mission Profile for TEA.

Table 2: Power required for each phase of flight of TEA

Flight Phase	Power Required [KW]
Take-off	917
Cruising	376
Sustained Load of 1.95 g	947
Max Speed	512
Maximum Power Available	1000

maximum available power.

E. Constraint Analysis

Figure 9 shows the constraint diagram for TEA. The abscissa is the wing loading, and the ordinate is the power-to-weight ratio (PWR). The PWR curves for different operations (including takeoff, cruising at design speed, cruising at maximum speed, and operation at sustained loading) are also shown in the figure. With a selection of wing loading, the maximum PWR shall satisfy the requirements of all operations. Also, landing is another limiting factor that sets

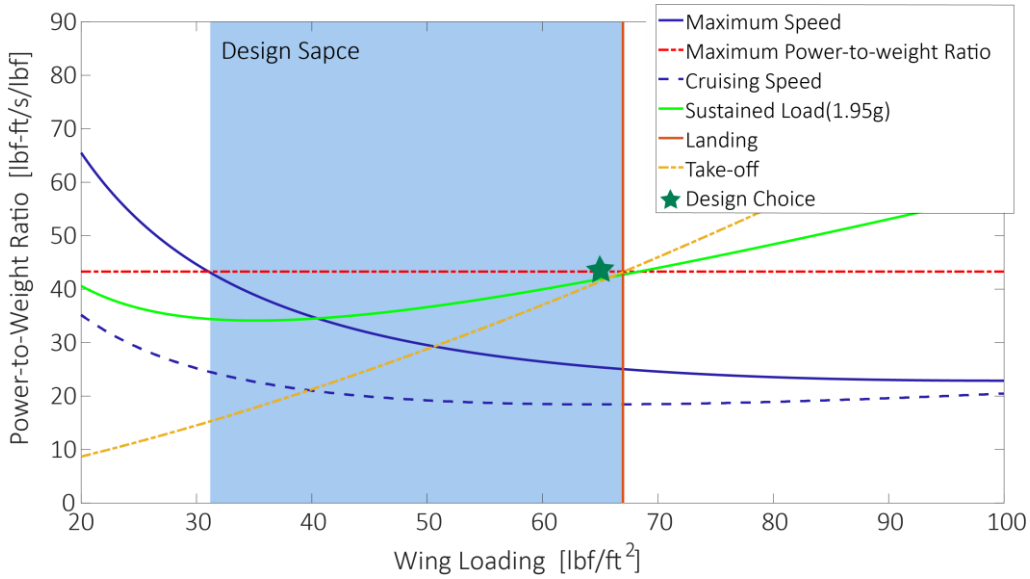

Figure 9: Constraint Diagram of TEA-10

the maximum wing loading, as indicated by the solid vertical line in Fig. 9. The maximum wing loading is determined by the landing velocity of the aircraft, which is 1.3 times the stall speed according to FAA regulations. The final design choice of TEA, indicated by the green star in the figure, falls in the design space of wing loading and has a PWR satisfied all operations. Though not presented in this section, a detailed procedure for the constraint analysis is included in Appendix B.

Lastly, a stability analysis of the airplane was considered. However, because of the joint wing design, the downwash effect on the aft wing cannot be assumed negligible. Without a detailed investigation of the joint wing's aerodynamics, the stability analysis is irrelevant. Therefore, the results from the stability analysis are not included.

IV. Discussions and Conclusions

The final design of the 10-passenger thin-haul electric plane (TEA-10) is competitive compared to aircraft of similar capacity, as shown in Table 3. Compared to the regular powered benchmarking target of PC24, TEA-10 has a lower cruising speed and payload capacity. However, the cruising speed has a small impact on its overall performance since the flight time is quite short, less than 150 minutes. Compare to the fully electric Eviation Alice, TEA-10 has a higher MTOW but offers more space in the cabin. In addition, TEA-10 allows operation on both paved and unpaved runways. It requires a runway at least 3200 feet long, for both paved and unpaved, to operate under all weather conditions, and operation on paved runways during good weather can be as short as 2200 feet. This enables the operation of TEA-10 at most airports. For instance, there are a total of 141 runways for the operation of fixed-wing ground-based aircraft in Indiana, and TEA-10 can operate on 98 of them under all weather conditions and even more in good weather conditions [23]. It can significantly reduce the travel time to airports as well as the administration time at large, hub airports.

Table 3: Comparison of TEA with Other Benchmarking Targets.

	PC24 [9]	Zunum ZA10	Eviation Alice	TEA-10
Capacity	8+2	10+2	9+2	10+2
Range [nm] (Max Loading)	2,000	610	540	500
Cruising Speed [KTAS]	440	295	240	245
MOTW [lb]	18,300	11,500	14,000	15,400
Propulsor	Twin Turbofans	Twin EDF	Triple Electric Propellers	Twin EDF
Energy Pack Weight Percent	33% Fuel	20% Battery 7% Fuel	60% Battery	51% Battery

In addition, the operation cost of TEA-10 is significantly reduced. The batteries on the TEA-10 have a total capacity of 1,080 KWh. Based on data from the US Energy Information Administration, the average price for electricity in transportation usage is 9.29 cents per KWh in May 2020 [24]. As a result, the operational fuel cost for TEA-10 is roughly 1.74 cents per seat mile. Compared to the 2.80 cents per seat mile as the average fuel expense of all U.S. airlines in 2019 [25], a potential 40% reduction in fuel cost is expected. Considering that aircraft operating thin-haul missions usually have a higher fuel cost per seat mile due to the lower fuel efficiency compared to the commercial airlines, the TEA-10 offers a significant advantage in operational cost. Also, a lower maintenance cost for the TEA-10 is expected considering the absence of hot parts (such as turbine blades) and its associated systems (such as fuel system) found in conventional jet engines.

The analysis showed that the battery energy density is still the bottleneck for all-electric aircraft design. For instance, it will be very challenging to meet the design requirement for the TEA-10 with the current state-of-art battery technology (200 Wh/kg); hence the weight of the airplane will likely exceed the maximum weight requirement for general aviation aircraft. The low battery density requires a high battery weight percentage. The propulsors may not be able to provide enough power to fly the required missions since the MTOW increases with the increased battery weight percentage using the 200 Wh/kg battery density. Even with the 300 Wh/kg battery density, the high battery weight percentage brings the most challenges of TEA-10. On the other hand, with continuous advances in battery technology, future airplanes can utilize less battery for the same mission requirement or provide an extended range with the same amount of battery, as shown in Fig. 10. With the same amount of battery, the range of the TEA-10 is approximately 750 nm at a 400 Wh/kg battery density. In the trade study, the analysis indicates that a higher aspect

ratio is beneficial for the TEA-10 design because of the associated improvement in the lift-to-drag ratio. However, an increase in aspect ratio adds a challenge to the structural integrity of the wing design and can increase weight. Therefore, a high-lift wing system, such as the distributed propulsion system demonstrated on the NASA X-57 Maxwell, can be beneficial for fully electric airplanes.

Furthermore, for the design of all-electric regional airplanes such as Embraer ERJ family and Bombardier CRJ family aircraft, a brief study using the same design program indicates that the design of such an aircraft (capacity of 50 passengers and a range of 1000 nm) can be very challenging but is possible at the battery power density of 500 Wh/kg. However, the time frame for the availability of 500 Wh/kg level battery technology is not entirely clear. More research is required to accelerate the development of battery technology.

To conclude, the conceptual design of a thin-haul electric aircraft was successfully carried out in the present study using current aircraft technology. The aircraft falls in the category of general aviation, according to the FAA regulations. It features a joint-wing design for better aerodynamic performance and is powered by two newly designed duct fans. The maximum takeoff weight (MTOW) of the airplane is 15,400 lbs. The cruise speed is Mach 0.42 at an altitude of 30,000 ft. To achieve the range requirement, the battery weight takes approximately 51% of MTOW, assuming a battery density of 300 Wh/kg. Both battery and high-efficiency aerodynamic structures, such as a high aspect ratio wing or joint wing, are essential for all-electrical aircraft design. In the foreseeable future, a Thin-Haul Electric Aircraft for private usage and on-demand commercial flight could be a reality in this coming decade.

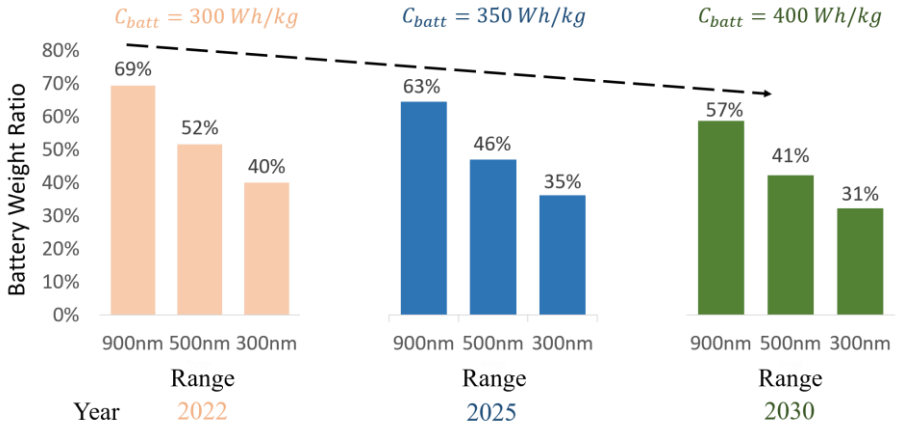

Figure 10: Change of battery weight percentage with changes in range and battery power density

Appendix A: Modified FLOPS Weight Estimation

The following weight estimation method is modified based on the FLOPS weight estimation method. Modifications are made due to the application of composite material, the electrical propulsion system, and advanced avionics. FLOPS weight estimation methods start with a designed gross weight, DG. The design gross weight is estimated at 15,000 lb based on the designed MTOW of Alice. DG will be updated to match design MTOW after the designed MTOW is estimated. Therefore, the reference wing area (*S.W.*) is founded as Equation A1, and wingspan (*SPAN*) is founded in Equation A2:

$$SW = DG/WSR \tag{A1}$$

$$SPAN = \sqrt{AR \times SW} \tag{A2}$$

The project uses the simplified wing weight estimation of FLOPS, which uses an equivalent bending material factor for calculation. The equivalent bending material (*B.T.*) is calculated as Equation A3.

$$BT = \frac{0.125 \times (0.37 + 0.7 \times TR) \times \left(\frac{SPAN^2}{SW}\right)^{EMS}}{CAYL \times TCA} \tag{A3}$$

where
E.M.S. = Wing strut bracing factor, which is 1.0 since no wing strut at the initial conventional design
C.A.Y.L. = Wing sweep factor, defined below in Equation A4
T.C.A. = Weighted average of the wing thickness to chord ratio, assumed as 0.08

$$CAYL = (1.0 - SLAM^2) \times (1.0 + C6 \times SLAM^2 + 0.03 \times CAYA \times C4 \times SLAM) \quad \text{(A4)}$$

where
SLAM = Sine of the ¾ chord wing sweep angle, calculated using Equation A5
C4 = Factor defined as Equation 6
C6 = Factor defined as Equation 7
CAYA = Factor defined as Equation 8

$$SLAM = \frac{TLAM}{\sqrt{1.0 + TLAM}} \quad \text{(A5)}$$

where
T.L.A.M. = Tangent of ¾ chord wing sweep angle, calculated using Equation A6

$$TLAM = \tan(SWEEP) - \frac{2.0 \times (1.0 - TR)}{AR \times (1.0 + TR)} \quad \text{(A6)}$$

$$C4 = 1.0 - 0.5 \times FAERT \quad \text{(A7)}$$

F.A.E.R.T. is defined as the Aeroelastic tailoring factor of the wing, varies from 0.0, no aeroelastic tailoring to 1.0, maximum aeroelastic tailoring. Defined as 0.5 for TEA-10

$$C6 = 0.5 \times FAERT - 0.16 \times FSTRT \quad \text{(A8)}$$

$$CAYA = AR - 5, \qquad for\ AR > 5 \quad \text{(A9)}$$

Then, the total wing bending material weight (*W1NIR*) for a fixed-wing single body general aviation aircraft is defined as Equation A10:

$$W1NIR = 30.0 \times BT \times ULF \times SPAN \times (1.0 - 0.4 \times FCOMP) \times (1.0 - 0.1 \times FAERT) \times \frac{PCTL}{1{,}000{,}000} \quad \text{(A10)}$$

where
ULF = Structural ultimate load factor, set to be 1.5 for TEA-10, according to C.F.R. §23.2230, which regulated the limit and ultimate loads of general aviation aircraft.
F.C.O.M.P. = Composite utilization factor for the wing structure; ranged from 0.0, no composite material used, to 1.0, maximum composite usage. Set to 0.3 for TEA-10 since the usage of composite material on the wing of a small airplane is limited due to sizes.
P.C.T.L. = Faction of the load carried by the defined wing, since the joint-wing design, with no horizontal tail at all, will be implied later, *P.C.T.L.* is set to be 1.0, which means 100% load is carried by the main wing.

The total wing shear material and control surface weight (*W2*) of TEA-10 is expressed as follow:

$$W2 = 0.25 \times (1.0 - 0.17 \times FCOMP) \times SFLAP^{0.5} \times DG^{0.5} \quad \text{(A11)}$$

where
S.F.L.A.P. is the total moveable wing surface area, including flaps, elevator, spoilers, etc. For TEA-10, set to 20% of the total wing area, expressed as $0.2 \times SW$

The total wing miscellaneous items weight for TEA-10 is roughly estimated in Equation A12 as:

$$W3 = 0.160 \times (1.0 - 0.3 \times FCOMP) \times SW^{1.20} \quad \text{(A12)}$$

The wing bending material weight inertia relief adjustment is used to adjust the weight of wing bending material calculated using Equation A13 to get the total bending material weight of the wing (*W1*) for TEA-10 is expressed as:

$$W1 = \frac{DG \times W1NIR + W2 + W3}{1.0 + W1NIR} - W2 - W3 \quad \text{(A13)}$$

The term of propulsion system pod inertia relief factor (*C.A.Y.E.*) is eliminated since all two E.D.F. is mounted on the rare of the fuselage.

The **Total Wing Weight** (*W.W.I.N.G.*) is defined as Equation A14:

$$WWING = W1 + W2 + W3 \quad \text{(A14)}$$

The **Fuselage Weight** of TEA-10 is defined as Equation A15:

$$WFUSE = 0.052 \times SWFUS^{1.086} \times (ULF \times DG)^{0.177} \times \mathrm{QCRUS}^{0.241} \times 0.8 \quad \text{(A15)}$$

where

A fudge factor of 0.8 is applied to the equation, represents a 20% structure weight reduction on the fuselage with the application of composite material in structure, which is foreseeable based on the weight reduction by using composite material on Boeing 787 [26].

S.W.F.U.S. is the fuselage wetted area ft^2, estimated as $\mathrm{SWFUS} = 3.14159 \times (\frac{XL}{DAV} - 1.7) \times \mathrm{D.A.V.}^2$

Q.C.R.U.S. is the cruise dynamic pressure in *psf*, estimated as Equation 16:

$$QCRUS = 1481.35 \times DELTA \times VCMN^2 \quad \text{(A16)}$$

where

DELTA is the ratio of pressure at cruise altitude to the pressure at sea level

The **Landing Gear Weight** of TEA-10 is expressed as the sum of the nose and main landing gears weight, as in Equation A17 and A18, respectively.

$$WLGN = 0.048 \times WLDG^{0.67} \times (0.525 \times XL)^{0.43} \quad \text{(A17)}$$

W.L.D.G., Aircraft design landing weight, is equal to the design gross weight *D.G.*, assume the weight of battery remains constant during the flight.

$$\mathrm{WLGM} = 0.0117 \times \mathrm{WLDG}^{0.95} \times (0.75 \times XL)^{0.43} \quad \text{(A18)}$$

The tail for TEA-10 is designed to be a V-tail section, which is hard to model using the FLOPS model. However, according to Raymer's, the total wetted area of V-tail need to be equal to the equal to the separated horizontal and vertical tail design in order to achieve the same stability and controllability. As a result, the tail section weight is modeled as a conventional tail with the same total wetted area. V-tail does require a more complex control system, and it will be dressed in the control system weight. Since the tail will need to bear more strain due to the joint wing design, the ultimate loading factor for the tail section is adjusted to 2.25. The **Tail Weight** is then expressed as the sum of the weight of the horizontal tail and vertical tail, **W.H.T.** and **W.V.T.**, expressed as Equation A19 and A20 respectively:

$$WHT = 0.016 \times SHT^{0.873} \times (ULFT \times DG)^{0.414} \times QCRUS^{0.122} \quad \text{(A19)}$$

where

S.H.T. = Horizontal tail theoretical area in ft^2, estimated as $SHT = 10 \times \frac{SW^2}{SPAN}$ based on the geometric parameter of TEA-10 and historical data.

U.L.F.T. = Tail ultimate loading factor, defined as 2.25

$$\mathrm{WVT} = 0.073 \times (ULFT \times DG)^{0.376} \times QCRUS^{0.122} \times SVT^{0.873} \times \left(\frac{ARVT}{CSVT^2}\right)^{0.357} / (\frac{100 \times TCVT}{CSVT})^{0.49} \quad \text{(A20)}$$

where

SVT = Vertical tail theoretical area in ft^2, estimated as $SVT = 0.0015 \times SW \times SPAN$

A.R.V.T. = Vertical tail theoretical aspect ratio, defined as 4.0 for TEA-10

$CSVT = \cos(SWPVT)$, where S.W.P.V.T. is vertical tail sweep angle at the quarter chord in *deg,* determined initially as -15 *deg*

T.C.V.T. = Vertical tail thickness to chord ratio, defined as 0.07 for TEA-10

The propulsion system of TEA-10, as discussed previously, is selected as two newly designed E.D.F. With only two propulsors, the **Weight of the Propulsion System** can be defined as the estimated weight of E.D.F.s, which roughly estimated as 500 lb each, expressed as Equation A21. The control system, including electric bus and other electrical components for the EDF.s, are either dressed in the electric and control system or assumed to be included in the propulsion system weight.

$$\mathrm{WMOT} = 500 \times 2 \tag{A21}$$

The equation for the **Surface Controls Weight** was obtained from the General Aviation Synthesis Program to FLOPS, and expressed as Equation A22:

$$\mathrm{WSC} = 0.404 \times \mathrm{SW}^{0.317} \times \left(\frac{DG}{1000}\right)^{0.602} \times ULF^{0.525} \times (1481.35 \times DELTA \times VMAX^2)^{0.345} \tag{A22}$$

The **System and Equipment Weight** equations in FLOPS are used for both general aviation and transport aircraft. Although the equations proved to be realistic for transport aircraft, some of them are failed to provide a reasonable estimation of the system and equipment weight based on the historical data of general aviation airplanes. The difference between the estimation and historical data can differ by up to 50% and more. The general aviation, which is usually lighter, has a less complicated system and few types of instruments compared to the transport aircraft, which were designed for long-range missions with high compacity. As a result, the equation for the weight of Instruments, Electrical, and Avionics are applied with a fudge factor of 0.6, and the modified equations had results closer to the historical data. Note that TEA-10 is designed using a fly-by-wire system. As a result, the hydraulic weight is neglected.

The **Instruments Weight** for TEA-10, which designed to have two flight crew, can be expressed as Equation A23:

$$\mathrm{WIN} = 8.64 \times (\mathrm{XL} \times \mathrm{WF})^{0.57} \times \mathrm{VMAX}^{0.5} \times 0.6 \tag{A23}$$

For the **Electrical System Weight**, the equation applies another fudge factor of 1.2 to address the increase of weight in the electrical system due to the usage of electrical propulsor and fly-by-wire system. However, this number is based on rough estimations and should be updated when more electrical airplanes are introduced. With ten passengers, the electrical weight can be expressed as Equation A24:

$$\mathrm{WELEC} = 163.67 \times XL^{0.4} \times WF^{0.14} \times 0.6 \times 1.2 \tag{A24}$$

Avionics Weight of TEA-10 is expressed in Equation A25:

$$WAVONC = 25.67 \times DESRNG^{0.1} \times (XL \times WF)^{0.43} \times 0.6 \tag{A25}$$

where

D.E.S.R.N.G. is the designed range for TEA-10, which is 500 *nm.*

The **Furnishing and Equipment Weight** of the cabin is expressed in Equation A26. A fudge factor of 0.8 was applied to the equation, indicated a 20% weight reduction in furnishing by using less furnishing, for example, less decoration in the cabin.

$$\mathrm{WFURN} = [694 + 2.6 \times \mathrm{XLP} \times (\mathrm{WF} + \mathrm{DF})] \times 0.8 \tag{A26}$$

The **Air Conditioning System Weight** is determined by Equation A27:

$$\mathrm{WAC} = (3.2 \times (\mathrm{XL} \times \mathrm{DF} \times \mathrm{WF})^{0.6} + 60.85) \times \mathrm{VMAX} + 0.075 \times \mathrm{WAVONC} \tag{A27}$$

Anti-Icing equipment is not required on the general aviation aircraft. However, TEA-10 includes the anti-icing equipment to enhance the safety of operation. The **Weight of Anti-Icing** equipment is expressed as Equation A28, assume the EDF has a diameter of 40 *in*:

$$\mathrm{WAI} = \frac{SPAN}{\cos(SWEEP)} + 28.5 + 1.5 \times WF \tag{A28}$$

The **Total Structural Weight** is expressed as Equation A29:

$$\mathrm{WSTRUC} = \mathrm{WFUSE} + \mathrm{WLGM} + \mathrm{WLGN} + \mathrm{WWING} + \mathrm{WHT} + \mathrm{WVT} \tag{A29}$$

Moreover, the **Total Equipment Weight** is expressed as Equation A30:

$$\mathrm{WEQP} = \mathrm{WELEC} + \mathrm{WAVONC} + \mathrm{WSC} + \mathrm{WHYD} + \mathrm{WIN} + \mathrm{WAC} + \mathrm{WAI} \tag{A30}$$

Appendix B: Constraint Analysis

The constraint analysis is performed based on the power available and power required to complete each task. The master constraint equation, developed from Conservation of Energy, can be expressed as Equation B1. The constrain plots are generated based on Max Speed, Sustained Loading, Take-off, and Landing, by varying wing loading (*W.S.R.*) value. Constrain for landing and takeoff performance was expressed as Equation B1 and B2, respectively.

$$\frac{P}{MTOW} = \frac{1}{\eta_{EDF}}\left[\frac{0.5 \times \rho \times {V_\infty}^3 \times C_{D0}}{WSR_c} + \frac{k_1 \times n^2 \times WSR_c}{0.5 \times \rho \times V_\infty} + k_2 \times n \times V_\infty + P_s\right] \tag{B1}$$

where

ρ is the atmospherical density, at cruising height for the max speed and sustained loading constraint,
n is the sustained loading factor, equal to 1 at max speed and designed load factor for sustained loading constraint,
WSR_c is the independent variable for this equation
and P_s, excess power, defined as:

$$P_s = \frac{V}{g} \times \frac{dV}{dt} + \frac{dh}{dt}$$

V is the speed of TEA-10 at that mission, $\frac{dV}{dt}$ is the rate of change of the speed, and $\frac{dh}{dt}$ is the rate of change of altitude.

$$WSR_{LD} = \rho_{GD} \times g \times S_L \times \left(\frac{C_{D0}}{2} + \frac{C_{L_{max,LD}}}{1.69} \times 0.4\right) \tag{B2}$$

where

WSR_{LD} is the wing loading resulted by the landing
S_L is the distance of the required landing runway

$$\frac{P}{MTOW} = \frac{(1.2)^3}{\eta_{EDF}} \times \sqrt{\frac{WSR_c}{\rho_{GD} \times {C_{L_{max,TO}}}^3}} \times \left(\frac{WSR_c}{\rho_{GD} \times g \times S_{TO}} + \frac{C_{D0}}{2} + \frac{\mu_{RTO} \times C_{L_{max,TO}}}{1.44}\right) \tag{B3}$$

Since the maximum power of the E.D.F. and MTOW knew, the maximum Power-to-weight ratio of TEA-10 is fixed, as well as the predefined *W.S.R*. As the design of TEA-10 located at the point of the maximum Power-to-weight ratio and designed *W.S.R.*, all lines of constraint should either be on the right side or below the point of the design on the constraint diagram.

Acknowledgments

This work began as a project supported by the Summer Undergraduate Research Fellowship program at Purdue University, West Lafayette. The authors thank Prof. William Crossley and his Ph.D. student Brandon Sell from the School of Aeronautics and Astronautics at Purdue University for supporting this project by providing valuable suggestions and ideas on the encountered problems. In addition, we thank Dr. James Mayhew at Rose-Hulman Institute of Technology on the lecture and notes of Aircraft Design, which was essential for this project.

References

[1] German, B.J. "Thin-Haul Aviation Operation Study." *On-Demand Mobility and Emerging Technology Joint NASA-FAA Workshop,* March 8, 2016, Arlington, VA. N.A.S.A. Strategic Framework for On-Demand Air Mobility

[2] "Climate Change," International Air Transportation Association (ITAT), URL: https://www.iata.org/en/programs/environment/climate-change/ [cited 20 July 2020]

[3] "Trends in Emissions that affect Climate Change," International Civil Aviation Organization, URL: https://www.icao.int/environmental-protection/Pages/ClimateChange_Trends.aspx [cited 20 July 2020]

[4] Brelje, B.J., and Martins, J.R.R.A., "Electric, hybrid, and turboelectric fixed-wing aircraft: A review of concepts, models, and design approaches," *Progress in Aerospace Sciences*, Vol. 104, Jan. 2019, pp. 1-19.

[5] Misra, A. "Summary of 2017 N.A.S.A. Workshop on Assessment of Advanced Battery Technologies for Aerospace Applications," GRC-E-DAA-TN51429, 2018. Available at http:// nrts.nasa.gov

[6] Kruger, M., Byahut, S., Uranga, A., Dowdle, A., Gonzalez, J., Hall, D.K., "Electrified Aircraft Trade-Space Exploration," *AIAA AVIATION Forums,* June 25-29, 2018, Atlanta, Georgia, 2018 Aviation Technology, Integration, and Operations Conference.

[7] "Eviation Alice Commuter," URL: https://www.eviation.co/alice/ [cited 2 August 2019]

[8] "Zunum Aero Aircraft," URL: https://zunum.aero/aircraft/ [cited 2 August 2019]

[9] "Pilatus PC12 NG" URL: https://www.pilatus-aircraft.com/en/fly/pc-12 [cited 2 August 2019]

[10] "Pilatus PC24" URL: https://www.pilatus-aircraft.com/en/fly/pc-24 [cited 2 August 2019]

[11] "King Air 350i" URL: https://beechcraft.txtav.com/en/king-air-350i [cited 2 August 2019]

[12] Code of Federal Regulations, Title 14 – Aeronautics and Space (2019), accessed via e-CFR

[13] Raymer, D.P., *Aircraft Design: A Conceptual Approach,* 5th edition, A.I.A.A. Education Series, A.I.A.A., Reston, Virginia, 2012

[14] "OpenVSP", URL: http://openvsp.org/ [cited 15 June 2020]

[15] Fielding. J.P., *Introduction to Aircraft Design,* Second edition, Cambridge University Press, One Liberty Plaza, New York, NY, 2017

[16] Lou, F., and Key, N.L. "Aerodynamic Design of a High-Efficiency Propulsor for a 10-Passenger Regional Electric Aircraft", School of Mechanical Engineering, Purdue University, West Lafayette, Indiana, 2019

[17] Dowdle, A.P., Hall, D.K., and Lang, J.H., "Electric Propulsion Architecture Assessment via Signomial Programming" *A.I.A.A. Propulsion and Energy Forum*, July 9-11, 2018, Cincinnati, Ohio, 2018 AIAA/IEEE Electric Aircraft Technologies Symposium

[18] Cuerno-Rejado, C., Alonso-Albir, L., Gehse, P., "Conceptual design of a medium-sized joined-wing aircraft," *Proceedings of the Institution of Mechanical Engineers, Part G: Journal of Aerospace Engineering,* Vol. 224, Issue 6, 2010, pp. 681-696

[19] Garica-Benitez, J., Cuerno-Rejado, C., Gomez-Blanco, R., "Conceptual design of a nonpolar wing airliner," *Aerospace Science and Technology,* Vol. 88, July 2016, pp. 561-571

[20] Wells, D.P., Horvath, B.L., and McCullers, L.A., "The Flight Optimization System Weight Estimation Method," N.A.S.A./TM-2017-219627/Volume 1. Available at http:// ntrs.nasa.gov

[21] Torenbeek, E., *Synthesis of Subsonic Airplane Design: An Introduction to the Preliminary Design of Subsonic General Aviation and Transport Aircraft, with Emphasis on Layout, Aerodynamic Design, Propulsion, and Performance,* 1982 Edition, Springer Science+Business Media B.V., 1982

[22] Brandt, S.A., Stiles, R.J., Bertin, J.J., Whitford, R. *Introduction To Aeronautics: A Design Perspective,* Second Edition, A.I.A.A. Education Series, A.I.A.A., Reston, Virginia, 2004

[23] "Airport Data & Contact Information," Federal Aviation Administration, URL: https://www.faa.gov/airports/airport_safety/airportdata_5010/menu/#datadownloads [cited 20 June 2020]

[24] "Average Price of Electricity to Ultimate Customers by End-Use Sector", U.S. Energy Information Administration, URL: https://www.eia.gov/electricity/monthly/epm_table_grapher.php?t=epmt_5_6_a [cited 22 July 2020]

[25] Airline Data Project, "Expense & Related: Fuel Expense per A.S.M.," Global Airline Industry Program, Massachusetts Institute of Technology, URL: http://web.mit.edu/airlinedata/www/2019%2012%20Month%20Documents/Expense%20Related/Fuel/Fuel%20Expense%20per%20ASM.htm [cited 22 July 2020]

[26] Hale, J., "Boeing 787 from the Ground Up", *AERO Magazine*, Issues 24, Quarter 04, 2006, pp. 16-24. URL: https://www.boeing.com/commercial/aeromagazine/articles/qtr_4_06/article_04_1.html [cited 15 June 2019]